Article

Prediction Model of Lean Coal Adsorption of Power Plant Flue Gas

Miaoxin Cheng, Gang Bai,* Hongbao Zhao, Jinyu Li, Jun Su, Jue Wang, and Xun Zhang

Read Online

ACCESS | Metrics & More | Article Recommendations

ABSTRACT: To minimize errors in calculating coal flue gas adsorption capacity due to gas compressibility and to preclude prediction inaccuracies in abandoned mine flue gas storage capacity for power plants, it is imperative to account for the influence of compression factor calculation accuracy while selecting the optimal theoretical adsorption model. In this paper, the flue gas adsorption experiment of a power plant with coal samples gradually pressurized to close to 5 MPa at two different temperatures is carried out, and the temperature and pressure data obtained from the experiment are substituted into five different compression factor calculation methods to calculate different absolute adsorption amounts. The calculated adsorption capacities were fitted into six theoretical adsorption models to establish a predictive model suitable for estimating the coal adsorption capacity in power plant flue gas. Results reveal significant disparities in the absolute adsorption capacity determined by different compression factors, with an error range of 0.001278−7.8262 (cm^3/kg). The Redlich−Kwong equation of state emerged as the most suitable for the flue gas of the selected experimental coal sample and the chosen composition ratio among the five compression factors. Among the six theoretical adsorption models, the Brunauer−Emmett−Teller model with three parameters demonstrated the highest suitability for predicting the adsorption capacity of coal samples in power plant smoke, achieving a fitting accuracy as high as 0.9922 at 49.7 °C.
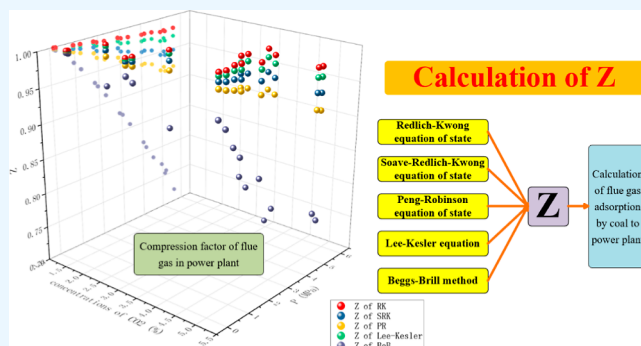
1. INTRODUCTION

With the escalating global greenhouse effect, population growth and urbanization are propelling the energy demand. Despite the development of renewable energy technologies, the predominant share of this demand still must be met by fossil fuels. More than 137 countries have set carbon neutrality targets. The International Energy Agency predicts that under the Sustainable Development scenario goal, the world will achieve net-zero emissions by 2070, and carbon capture, utilization, and storage will contribute to a cumulative carbon reduction of 15%.[1] Because of the depletion of coal resources and the continuous advancement of the global "carbon neutrality" plan, domestic and foreign coal mines are scaling back production or shuttering operations, rapidly increasing the number of closed/abandoned coal mines.[3] Flue gas constitutes the primary air pollutant in combustion power plants, including particulate matter, sulfur oxides, nitrogen oxides, and carbon dioxide.[2] In the face of the increasingly severe global greenhouse effect and the growing demand for clean energy, the absorption and storage of flue gas from abandoned mines are effective ways to solve the above problems. Given the challenges associated with treating power plant flue gas and its substantial impact on the greenhouse effect, injecting it into abandoned mines for CO_2 storage and facilitating the displacement of available energy CH_4 holds

practical significance. This approach is crucial for further realization of the goal of carbon neutrality.

Numerous scholars have extensively researched the adsorption of CH_4, CO_2, and N_2 by coal. Dutta et al. (2008)[4] discussed the CO_2 adsorption behavior of Illinois coal at medium pressure and fitted the adsorption calculation results with Langmuir and Dubinin−Astakhov adsorption models, but the fit with the D−A equation was better. Pan et al. (2009)[5] introduced the simulation work of adsorption models such as the extended Langmuir model, ideal adsorption solution model, and two-dimensional equation of state implemented in the coalbed methane reservoir simulator SIMED II. Sakurovs et al. (2012)[6] studied the adsorption of CO_2, CH_4, C_2H_6, and N_2 to some coals under 55 °C and 20 MPa pressure to clarify the relationship between the adsorption behavior of carbon dioxide and methane by coal under high pressure. The modified Dubinin−Radushkevich model is used to fit the adsorption isotherm. The results show

that the maximum adsorption capacity of coal for different gases is highly correlated. The relationship between the maximum adsorption capacity of coal to gas and its critical temperature is approximately proportional.

Lee et al. (2013)[7] studied the competitive adsorption behavior of CO_2/CH_4 on dry and wet anthracite under 318 and 338 K and 13 MPa pressures and compared the adsorption behavior with that of pure CO_2 and CH_4. Because the adsorption behavior of the CO_2/CH_4 mixture is similar to that of pure CO_2 at the same density, the fluid density in the free volume is an important variable to estimate the ECBM recovery efficiency effectively. Yang et al. (2019)[8] studied a comprehensive series of experiments to measure the fractal dimension of coal and its relationship with methane adsorption capacity. The thermodynamic gas adsorption model on heterogeneous surfaces is restudied, and a theoretical model between the fractal dimension and Langmuir constant is proposed. Qi et al. (2019)[9] explored the fluid distribution in the pores, revealing that temperature only changed the size of the adsorbed phase density, while the pore diameter not only altered the size but also influenced the trend of the adsorbed phase density with pressure. Finally, a temperature-dependent model is established. Based on this model, adsorption over a more comprehensive temperature range can be predicted. Meng et al. (2019)[10] delved into the adsorption behavior of supercritical CO_2 and CH_4 on three varying types of coal at different temperatures of 35 and 45 °C. The effects of temperature, pressure, and coal grade on Gibbs excess and absolute/actual adsorption capacity of coal samples in supercritical CO_2/CH_4 are analyzed. Several traditional isotherm models were applied to interpret the experimental data, and the Langmuir-related model was validated to provide good performance. Kang et al. (2019)[11] investigated the adsorption behavior of methane in six different types of coal, established a kinetic model to describe the changes in air pressure and heat release during the adsorption process and proposed corresponding isotherm models to characterize the adsorption amount and heat of pretreated and untreated coal samples.

Mu et al. (2019)[12] established a hydraulic-mechanical-thermal coupling numerical model for enhanced coalbed methane recovery (gas ECBM) by flue gas injection, which mainly considered the coupled gas—water two-phase flow, competitive adsorption, temperature change, and coal deformation. According to the model, a proper increase in flue gas injection temperature is conducive to the desorption of CH_4 adsorption and, thus, to the permeability and the CO_2 retention. Chen et al. (2021)[13] divided residual coal into loose and columnar residual coal and conducted gas adsorption experiments. The results show that in the range of 0.5—2.5 MPa, the methane adsorption capacity of loose residual coal can be reduced by 19.5% under strong coal supplement compared with that under progressive coal supplement. With the decrease of environmental pressure, methane adsorption by the briquette decreases Liu et al. (2021).[14] Under different gas pressures, the gas pressure is directly proportional to the initial gas adsorption rate, in line with the Langmuir adsorption theory, and a quadratic function relationship with the amount of unabsorbed gas.

When the gas pressure is higher than 2.4 MPa, the time required to reach adsorption equilibrium is reduced to 5 h. Liu et al. (2022)[15] proposed that in order to evaluate the in situ gas content, the excess adsorption amount must be calibrated to the absolute adsorption amount through mathematical correction. Therefore, based on the excessive isothermal adsorption experiment, the absolute adsorption isotherm was obtained by quantification of free methane and adsorbed methane using nuclear magnetic resonance, and the exact in situ density and volume of adsorbed methane were obtained during gas adsorption. Cheng et al. (2023)[16] systematically reviewed and summarized previous calculation methods of adsorbed phase density, encompassing the empirical method, indirect method, and direct method. A direct calculation method of adsorbed phase density considering multistage adsorption behavior was introduced in detail, and it was suggested that the van der Waals density should be used as the adsorbed phase density in the empirical method. Huang et al. (2023)[17] revealed the general rule of CO_2/CH_4 competitive adsorption behavior through molecular posture analysis. With the aid of molecular dynamics theory, a machine-learning algorithm is proposed to predict competitive adsorption behavior quickly and accurately, and the influencing factors are analyzed in detail.

The accurate analysis of the adsorption performance of coal to power plant flue gas and the prediction of the adsorption and storage of abandoned mine to power plant flue gas depend on the experimental method, the analysis of experimental data, and the selection of adsorption model in the isothermal adsorption experiment. At present, the research on coal adsorption of mixed gas is mainly focused on different experimental methods and molecular simulation, but the accuracy of coal adsorption of power plant smoke is rarely studied. Finding a suitable calculation model can improve the calculation accuracy of the gas adsorption amount, which is conducive to the analysis of experimental results and the accurate prediction of the gas adsorption sealing stock of the power plant in the later abandoned coal mine and provides better basic theoretical analysis for the calculation and prediction of coalbed methane mining. Because of the large space of abandoned mines, accurate calculation of coal adsorption capacity can reduce the space waste of abandoned mines and reduce the treatment cost of flue gas emissions of power plant. The compression factor Z is a correction factor that must be considered when the ideal gas equation of state is applied to the actual gas, which is used to represent the deviation in volume between the actual gas and the ideal gas after compression under the same pressure.[18] Therefore, the calculation of the actual gas is an extremely important problem in the calculation of the adsorption amount of coal in the flue gas adsorption experiment of a power plant.

2. EXPERIMENT AND THEORY

2.1. Sample Preparation. Coal samples were extracted from a location of 100 m into a tunnel 23,072, Zhaozhuang no. 2 Well, Changzhi City, Shanxi Province. Following extraction, the coal samples were hermetically sealed and stored in large blocks. Upon arrival at the laboratory, part of the coal sample was retained for industrial analysis according to <GB/T 30732-2014 Proximate analysis of coal by instrumental method>. The remaining large coal sample was decomposed into small coal sample and then ground into small particles with a pulverizing mill. The coal powder between 60 and 80 mesh is selected to prepare the coal sample with a particle size of 0.2—0.3 mm. It is convenient to carry out the adsorption experiment quickly and reduce the experiment period. In order to minimize the influence of water in the coal sample on the adsorption

Table 1. Industrial Analysis of a Coal Sample from Zhaozhuang no. 2 Well

sample	M_{ad} (air drying base moisture)	A_{ad} (ash)	V_{daf} (dry ash-free volatiles)	apparent relative density (g/cm³)	true relative density (g/cm³)	K (%) (the porosity)
Zhaozhuang no. 2 well	0.65	7.98	16.36	1.29	1.36	5.15
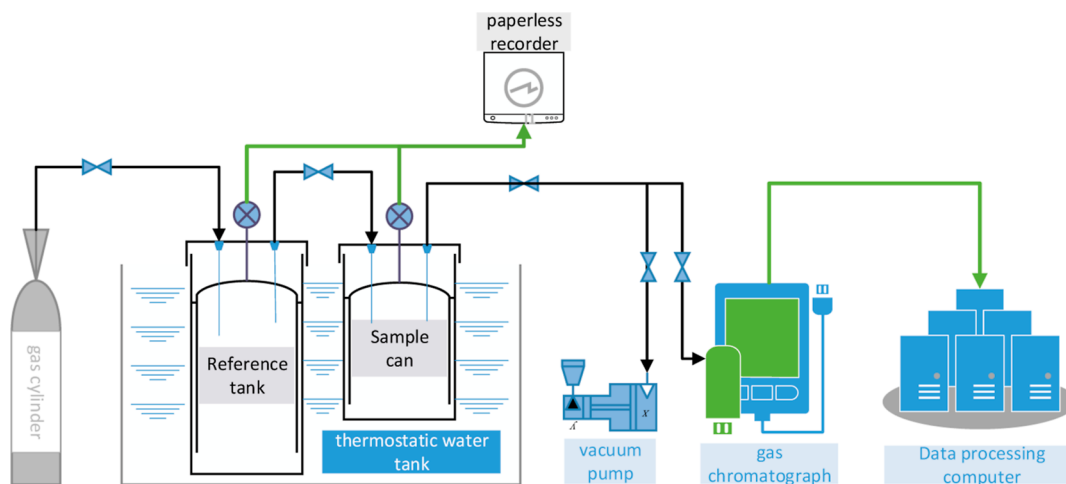
Figure 1. Schematic diagram of experimental apparatus.

experiment, we used a drying box to vacuum-dry the coal sample for 6 h at a temperature of 333.15 K to remove the original water in the coal sample. The industrial analysis results of coal samples are detailed in Table 1.

2.2. Experiment of Flue Gas Adsorption in a Power Plant. *2.2.1. Experimental Procedure for Adsorption Measurements.* The experiment utilized an independently constructed coal-to-gas adsorption device, the structure of which is illustrated in Figure 1. To meet the experimental constant temperature conditions, a constant temperature water bath is used to keep the ambient temperature of the tank constant. The data of gas pressure and temperature were collected in real time by the data processor above the tank, and the component proportion of the free mixed gas in the sample tank under adsorption equilibrium was analyzed by connecting a BFR-3420A gas chromatograph at the end of the experimental system. The gas used in the experiment is a mixture of N_2:78.5%, CO_2:16.5%, O_2:5%, which is configured to simulate the flue gas of the power plant according to the gas ratio measured in the field.

By reading the literature and combining with the actual situation in the coal mine, the ambient temperature of the experimental device was set at approximately 30 and 50 °C. The pressure of the control system was continuously pressurized to 5 MPa. Five nodes were selected to record the values of the adsorption amount under different pressure conditions to simulate the adsorption environment within the mine.

2.2.2. Computational Procedure for Adsorption Measurements. In this paper, the calculation process of flue gas adsorption capacity in a power plant is according to the national standard <NB/T 10019-2015 Experimental method of multicomponent gas isothermal adsorption on coal>. The calculation process of coal adsorption experiment for power plant flue gas is mainly as follows:

1. The volume of pipe is measured according to the gas equation of state V_C V_S

$$\begin{cases} \dfrac{P_C V_C}{Z_C} = \dfrac{P_h(V_C + V_S)}{Z_h} \\[2mm] \dfrac{P'_C V_C}{Z'_C} = \dfrac{P'_h(V_C + V_S - V_b)}{Z'_h} \end{cases}$$

V_c is the reference pipe and its pipe volume, V_s, is the sample tank and its pipe volume.

2. The volume of free space is calculated according to Boyle's law V_f

$$\frac{P_a V_C}{Z_a} = \frac{P_b(V_C + V_f)}{Z_b}$$

V_f is the volume of free space.

3. The number of adsorbed phase moles at each pressure point was calculated, n_{i+1}

$$n_{i+1} = n_i + \frac{V_r}{R}\left(\frac{P_{r1}}{Z_{r1}T_{r1}} - \frac{P_{r2}}{Z_{r2}T_{r2}}\right) + \frac{V_r}{R}\left(\frac{P_{s1}}{Z_{s1}T_{s1}} - \frac{P_{s2}}{Z_{s2}T_{s2}}\right)$$

n_{i+1} is the adsorption phase at each pressure point.

4. The relative adsorption volume of each pressure point is calculated, V'_g

$$V'_g = \frac{nRZ_{S2}T_{S2}}{P_{S2}}$$

V'_g is the relative adsorption volume.

5. The absolute adsorption volume at each pressure point is calculated, V_g

$$V_g = \frac{V'_g}{1 - \frac{\rho_f}{\rho_s}}$$

V_g is the absolute adsorption volume.

ρ_{free} in the above formula is the free phase density

$$\rho_f = \frac{MP_{SC}}{1000ZRT_{SC}}$$

ρ_s is the adsorption phase density

$$\rho_S = \frac{RT_C}{8P_C}$$

6 .The absolute adsorption capacity of each pressure point is calculated, V_{ad}

$$V_{ad} = \frac{V_g}{M}$$

V_{ad} is the absolute adsorption capacity.

Through the aforementioned experimental calculation process, it is found that the compression factor is a more important correction factor for the calculation of the adsorption amount of the coal adsorption mixed gas. It recurs frequently throughout the calculation process and exhibits variability in response to changes in the temperature, pressure, and gas composition. Since the calculation of the adsorption phase, the compression factor has appeared in the formula as an important correction variable, which affects the calculation of the final absolute adsorption step by step. The calculation of the adsorption phase involves four different compression factors, which vary with temperature and pressure. To increase the accuracy of prediction of coal's adsorption capacity of power plant flue gas, this paper considers the calculation error caused by the compression factor coefficient when calculating the absolute adsorption capacity of coal's adsorption capacity of power plant flue gas. Based on the selection of the optimal compression factor equation, the error of theoretical adsorption model selection and parameter determination for the prediction of adsorption capacity will be further increased.

2.3. Theoretical Framework. Due to disparities between the real gas and the ideal gas, the density compensation of the real gas can not only be compensated by the temperature and pressure compensation but also needs to provide the compensation of the compression factor. As a dimensionless parameter, the compression factor is a very important correction factor in the actual gas equation of state. The compression coefficient of the actual gas can be calculated according to the comparison temperature T_r and comparison pressure P_r. To calculate the compression factor of the mixed gas more accurately, this section combines the three gas state equations of Redlich−Kwong (RK), Soave−Redlich−Kwong (SRK), and Peng−Robinson (PR) with the actual gas state equation to obtain the compression factor calculation equation under different temperatures and pressures. Additionally, the chapter introduces the Lee−Kesler equations, known for their broad applicability, and compares them with the Beggs−Brill methods for a comprehensive assessment and calculation.

2.3.1. Actual Gas Equation of State. The Redlich−Kwong equation of state, or RK equation for short, is an equation of state based on van der Waals equation used to approximate the behavior of real gases in physical chemistry.[19] The Soave−Redlich−Kwong equation of state, or SRK equation for short, is a modified form of the RK equation of state and an approximate equation of state describing the behavior of real gases based on the van der Waals equation in physical chemistry. The SRK equation is used to calculate the volume of the gas phase and liquid phase by increasing the eccentricity factor to expand the scope of application. The Peng−Robinson

equation of state, referred to as PR equation, is one of the most widely used and accurate cubic *PVT* equation of state.[20] Since its official publication in 1976, it has been widely used in the field of the petrochemical industry. Because the flue gas calculated in this paper is a mixed gas, the Kay rule is used to calculate the critical condition of the mixed gas while calculating the compression factor.[21] Among them, Kay rule:

$$\omega = \sum_j x_j \cdot \omega_j \quad T_c = \sum_j x_j T_{cj} \quad P_c = \sum_j x_j \cdot P_{cj}$$

RK equation of state

$$P = \frac{RT}{V - b} = \frac{a}{T^{0.5} V(V + b)}$$

$$a = \frac{0.42748 R^2 T_c^{2.5}}{P_c} \qquad b = \frac{0.08664 R T_c}{P_c}$$

The RK equation of state is combined with the actual gas equation of state modified by the compression factor, and the actual gas equation of state is $pV = ZnRT$ where M is the molar mass of the gas, kg/mol; R is the universal gas constant $R = 8.3143$ J/(mol·K); P, T, and ρ represent the pressure (MPa), temperature (K), and density (kg/m^3) of the actual gas, respectively.

The RK equivalent substitution equation is

$$Z = \frac{h}{1 - h} - \frac{4.934}{T_r^{1.5}}\left(\frac{h}{1 + h}\right)$$

$$h = \frac{0.08664 R T_r}{P_r} \qquad T_r = \frac{T}{T_c} \qquad P_r = \frac{P}{P_c}$$

where Z is the compression coefficient of gas under temperature and pressure conditions, without dimension; h is the intermediate variable; T is the temperature of the gas, K; P is the pressure of the gas, MPa; T_r is the contrast temperature of the gas, K; P_r is the relative pressure of gas, MPa; T_c is the critical temperature of gas, K; and P_c is the critical pressure of gas (MPa).

The SRK equation of state is

$$P = \frac{RT}{V - b} = \frac{\alpha(T)}{V(V + b)} \qquad a = \frac{0.4274 R^2 T_c^2}{P_c}$$

$$b = \frac{0.08664 R T_c}{P_c}$$

$$\alpha(T) = ((1 + (0.48 + 1.574\omega - 0.176\omega^2))(1 - T_r^{0.5}))^2$$

where ω is the eccentric factor: $\omega = \frac{3}{7}\left(\frac{\theta}{1 - \theta}\right)\log P_c - 1$, including $\theta = \frac{T_b}{T}$

The SRK equivalent substitution equation is

$$Z^3 - Z^2 + (A - B - B^2)Z - AB = 0$$

$$A = \frac{aP}{R^2 T^2} \qquad B = \frac{bP}{RT}$$

$$a = 0.42748 \frac{R^2 T_c^2}{P_c}[1 + f(\omega)(1 - T_r^{0.5})]^2$$

$$b = \frac{0.08664 R T_c}{P_c}$$

$$f(\omega) = 0.48 + 1.574\omega - 0.176\omega^2$$

The PR equation of state is

$$P = \frac{RT}{V-b} - \frac{ac}{V(V+b)+b(V-b)}$$

$$a = \frac{0.457235R^2T_c^2}{P_c} \qquad b = \frac{0.77796RT_c}{P_c}$$

$$c = [1 + f(\omega)(1 - T_r^{0.5})]^2$$

$$f(\omega) = 0.37464 + 1.54226\omega - 0.26992\omega^2$$

The PR equivalent substitution equation is

$$Z^3 - (1-B)Z^2 + (A - 2B - 3B^2)Z - AB + B^2 + B^3 = 0$$

$$A = \frac{aP}{R^2T^2} \qquad B = \frac{aP}{RT}$$

$$a = \frac{0.457235R^2T_c^2}{P_c}[1 + f(\omega)(1 - T_r^{0.5})]^2$$

$$b = \frac{0.77796RT_c}{P_c}$$

2.3.2. Lee−Kesler Equation. The Lee−Kesler equation[22] has a high evaluation on its practicability in calculating compression factors and is currently recognized as a good estimation equation. It is applicable to both gas and liquid phases and is often used in engineering calculations.

The Lee−Kesler equation is

$$Z = Z^{(0)} + \frac{\omega}{\omega^{(r)}}(Z^{(0)} - Z^{(r)})$$

where $Z^{(0)}$ and $Z^{(r)}$ are calculated by the Virial equation

$$Z^i = \frac{P_r V_r}{Z_r} = 1 + \frac{B}{V_r} + \frac{C}{V_r^2} + \frac{D}{V_r^5} + \frac{c_4}{T_r^5 V_r^5}\left(\beta + \frac{\gamma}{V_r^2}\right)$$

$$\exp\left(-\frac{\gamma}{V_r^2}\right)$$

$$B = b_1 - \frac{b_2}{T_r} - \frac{b_3}{T_r^2} - \frac{b_4}{T_r^3} \quad C = c_1 - \frac{c_2}{T_r} + \frac{c_3}{T_r^2} \quad D$$

$$= d_1 + \frac{d_2}{T_r}$$

The values of the constants required in the formula are shown in Table 2.

Table 2. Required Constants for the Lee−Kesler Equation

constant	simple fluid (Ar)	reference fluid (C_8H_{18})
b_1	0.1181193	0.2026579
b_2	0.265728	0.331511
b_3	0.154790	0.027655
b_4	0.030323	0.203488
c_1	0.0236744	0.0313385
c_2	0.0186984	0.0503618
c_3	0.0	0.016901
c_4	0.042724	0.041577
$d_1 \times 10^4$	0.155488	0.48736
$d_2 \times 10^4$	0.623689	0.0740336
β	0.65392	1.226
γ	0.060167	0.03754

2.3.3. Beggs−Brill Method. Brill and Beggs in 1974 gave an exact formula for calculating the value of the *z*-factor, which can be used in many engineering calculations.

The Beggs−Brill method is

$$Z = A + \frac{1-A}{e^B} + CP_{pr}^D$$

In the formula, parameters *A−D* are the parameter values including P_{pr} and T_{pr}

$$A = 1.39(T_{pr} - 0.92)^{0.5} - 0.36T_{pr} - 0.1$$

$$B = (0.62 - 0.36T_{pr})P_{pr} + \left(\frac{0.066}{T_{pr} - 0.86} - 0.037\right)P_{pr}^2$$

$$+ \frac{0.32P_{pr}^6}{10^E}$$

$$C = 0.132 - 0.32\ln T_{pr} \qquad D = 10^F$$

$$E = 9(T_{pr} - 1)$$

$$F = 0.3106 - 0.49T_{pr} + 0.1824T_{pr}^2$$

where P_r is the pseudo-contrast pressure (ratio of pressure to pseudo-critical pressure) and T_r is the quasi-contrast temperature (the ratio of temperature to quasi-critical temperature).

$$P_r = \frac{P}{P_c} T_r = \frac{T}{T_c}$$

In the calculation process, the physical and chemical parameters of each single component gas that we need to use are listed in the following table.

3. RESULTS AND DISCUSSION

3.1. Adsorption Computational Analysis. The temperature and pressure data measured in the experiment were substituted into the compression factor calculation program developed in MATLAB to obtain the required compression factor values of power plant flue gas by using five compression factor calculation equations under different experimental environments. Subsequently, the obtained values for different compression factors were incorporated into the calculation of coal adsorption capacity for power plant flue gas, yielding the relevant values for the coal adsorption phase and absolute adsorption capacity of power plant flue gas. Refer to Tables 3 to 5 and Figures 2 to 7. The coal sample masses in the two groups of experimental sample tanks are 391.2 g at 29.4 °C and 388.4 g at 49.7 °C, respectively (see Figures 3−6).

Table 3. Physical and Chemical Parameters of Gas Required for the Experiment

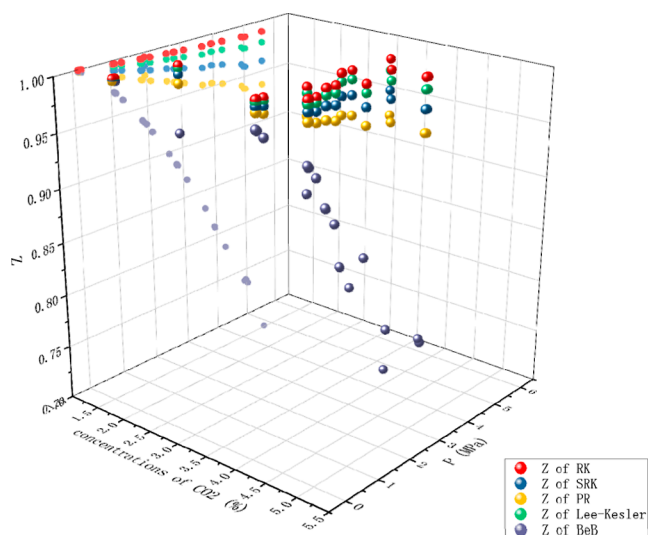|	He	CO_2	O_2	N_2
critical temperature (K)	5.25	304.45	154.2	126.1
critical pressure (MPa)	0.228994	7.39	5.08	3.4
boiling point (K)	4.25	194.65	90.05	77.35

It can be seen from Tables 3 and 4 that the difference between the adsorption amounts calculated under different compression factor calculation methods gradually expands with the expansion of measurement units. The Beggs−Brill method and the other four calculation methods have 2 to 5 times errors under different temperatures. The absolute adsorption volume
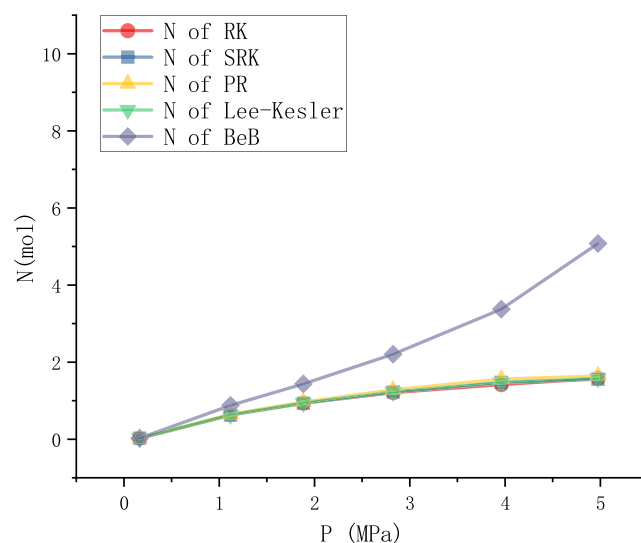
Table 4. Adsorption Phase and Absolute Adsorption Volume under Different Pressures at 29.4 °C

29.4 °C	adsorbed phase N (mol)				
P	RK	SRK	PR	LEE	BEB
0.168	0.0181	0.0181	0.0179	0.0177	0.0175
0.954	1.3167	1.3153	1.3477	1.3214	1.6677
1.946	2.276	2.2384	2.3079	2.2692	3.3675
3.04	3.2024	3.2191	3.3531	3.2341	5.3742
4.165	3.7924	3.9028	4.1028	3.8852	7.1717
4.957	4.0839	3.9465	4.1171	4.0511	9.3781

Table 5. Adsorption Phase and Absolute Adsorption Volume under Different Pressures at 49.7 °C

49.7 °C	adsorbed phase N (mol)				
P	RK	SRK	PR	LEE	BEB
0.163	0.0211	0.021	0.0209	0.021	0.0208
1.117	0.6295	0.6237	0.6423	0.6301	0.8748
1.882	0.9323	0.9288	0.9617	0.9373	1.4309
2.824	1.2043	1.2215	1.2772	1.2246	2.2034
3.959	1.4158	1.4716	1.5575	1.4625	3.3693
4.975	1.5719	1.553	1.6378	1.5796	5.0748

Figure 2. Z at 29.4 °C.

Figure 3. Z at 49.7 °C.

Figure 4. Relationship between P and N at 29.4 °C.

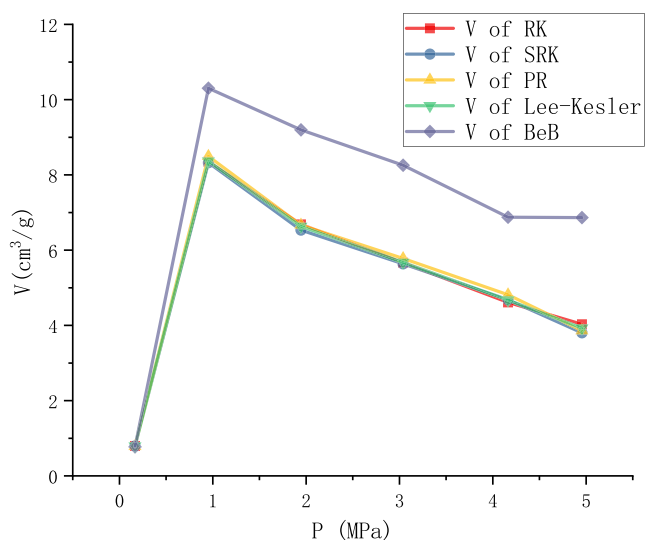**Figure 5.** Relationship between P and N at 49.7 °C.

error ranges of RK, SRK, PR, and LEE calculation methods are 0.069−0.226 at 29.4 °C and 0.004−0.0547 at 49.7 °C. This underscores the critical importance of selecting an appropriate compression factor calculation equation.

Figures 2 and 7 illustrate that the resulting errors between calculation methods of different compression factor coefficients gradually increase with the increase in pressure. At 4 MPa, the error in adsorption capacity calculated by the RK equation, SRK equation, PR equation, and Lee−Kesler equation is the largest. The trends of the adsorption phase and absolute adsorption capacity curves obtained by the five different compression factor calculation methods at two temperatures are roughly the same. The adsorption phases calculated by the ,RK equation, SRK equation, PR equation and Lee−Kesler equation all increase with increasing pressure. At 29.4 °C, the adsorption phase curve increases slowly with the increase in pressure after pressurization to 4 MPa. At 49.7 °C, the growth
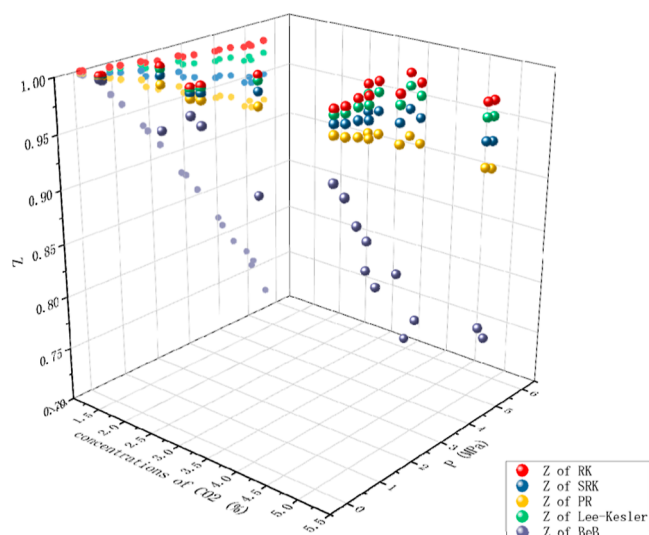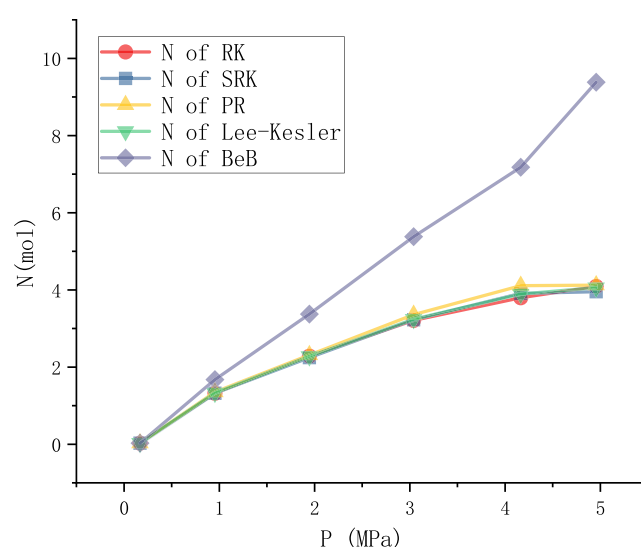
Figure 6. Relationship between P and V at 29.4 °C.
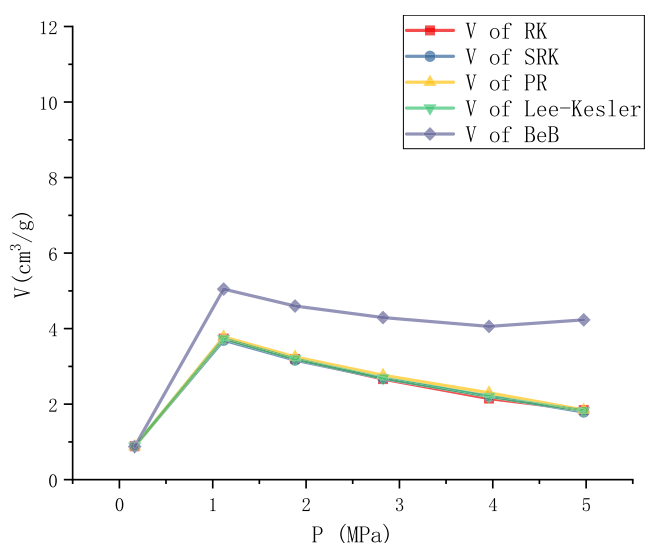
Figure 7. Relationship between P and V at 49.7 °C.

equations. The value is much higher than those of the other four equations.

3.2. Adsorption Model. The adsorption phase and adsorption volume, computed using data acquired from the aforementioned experiments under five different gas state equations, cannot be directly evaluated for proximity to the actual gas adsorption quantity. To ascertain the optimal adsorption simulation model for the coal sample, the results from the five calculation methods were substituted into six distinct adsorption models. MATLAB software was employed for data fitting. The selection of the most suitable compression factor calculation equation and theoretical adsorption model was based on the fitting accuracy, as determined by the coefficient of determination (R^2).

3.2.1. Adsorption Phase Fitting. First, different adsorption results were fitted using the Freundlich equation, and the obtained fitting parameters and results are shown in Table 5 and Figures 8−12. The Freundlich equation[23] is a relatively
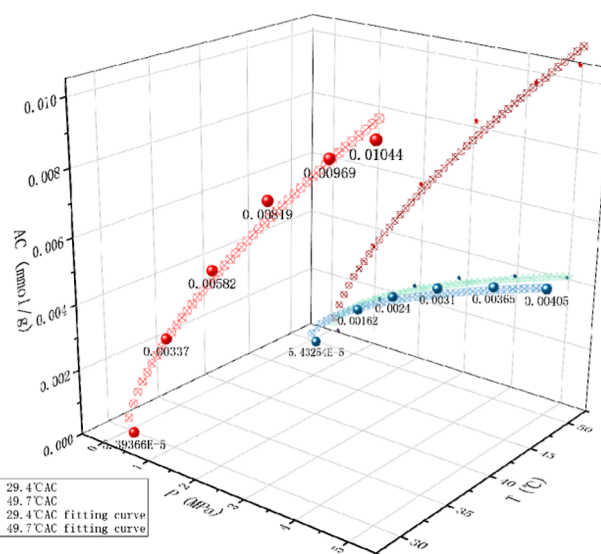

Figure 8. RK equation is used to fit F.

of the adsorbed phase curve starts to slow down with the increase in pressure after pressurization to 2 MPa.

The molar number and absolute adsorption capacity of the adsorption phase at 29.4 °C are significantly higher than that at 49.7 °C. With increasing pressure, the adsorption phase and absolute adsorption capacity at 29.4 °C are gradually higher than that at 49.7 °C. When approaching 5 MPa, the adsorption phase and absolute adsorption capacity at 29.4 °C are twice as high as those at 49.7 °C. Under the two experimental temperatures, the inflection point of the various compression factor calculation methods is evident, and the inflection point of both methods is about 1 MPa, where the trend changes from rising to decreasing. The inflection points of different temperature and compression factors are obvious. The inflection point is because of the existence of competitive adsorption in the process of coal adsorption of power plant flue gas. With the increase in pressure, the gas with stronger adsorption will replace the gas with weaker adsorption. The adsorption phase and absolute adsorption capacity obtained by the Beggs−Brill algorithm are different from the other four
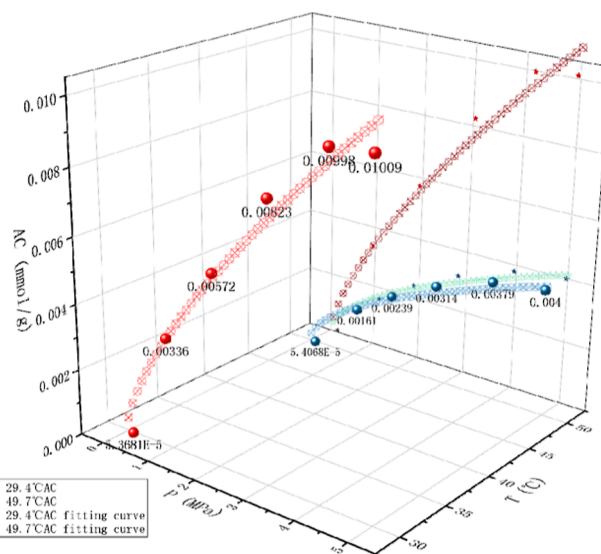

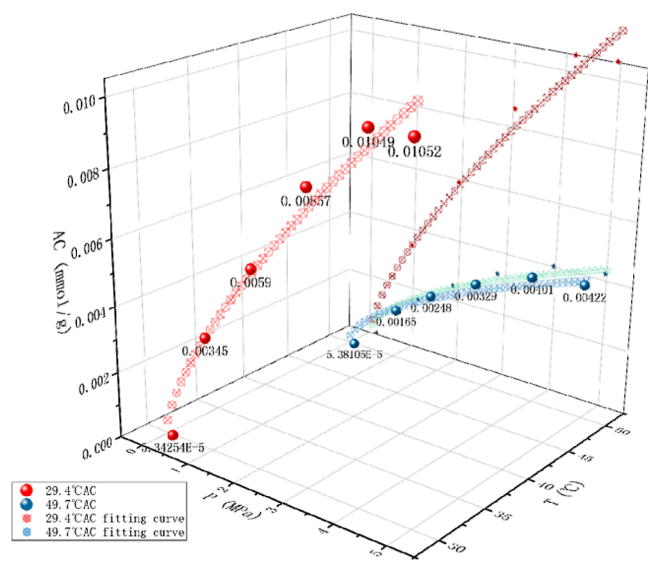**Figure 9.** SRK equation is used to fit F.

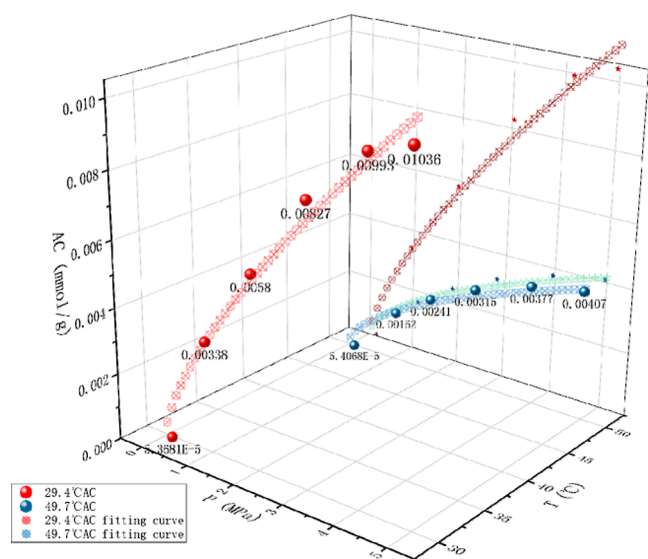**Figure 10.** PR equation is used to fit F.

Figure 11. LEE equation is used to fit F.

basic equation of state. It is of great significance for chemisorption. The Freundlich equation is referred to as the F equation in this paper, and its expression is as follows

$$N = \frac{x}{m} = kP^{1/a}$$

where N is the adsorption phase at adsorption equilibrium, mmol/g; x is the amount of adsorbed gaseous substances or the volume in a specific case, mmol; m is the quality of coal sample, g; k and a are constants determined by temperature, pore structure of the coal sample, and other factors. The adsorption phase at two different temperatures was substituted into the Freundlich equation and fitted with MATLAB. The fitting coefficients under different compression factor calculation methods are obtained.

Because the isothermal adsorption fitting curve of the Freundlich equation has the same trend as the coal-to-power plant flue gas adsorption phase point diagram, the fitting results of the coal-to-power plant flue gas adsorption phase are analyzed in this section. The adsorption phase is an important
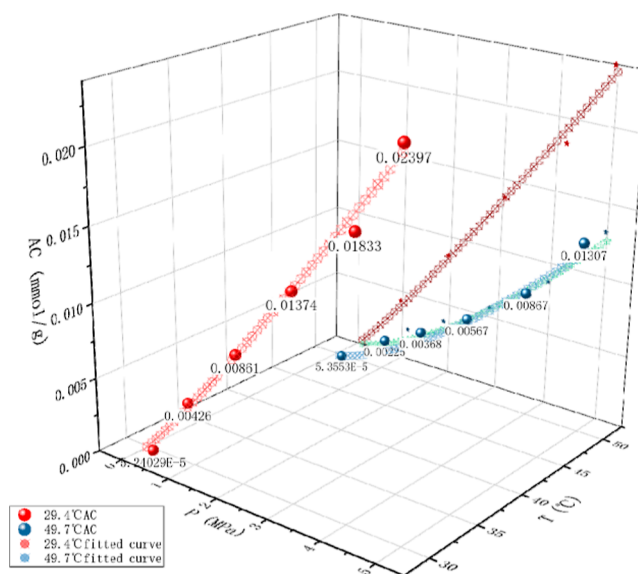

Figure 12. BEB equation is used to fit F.

intermediate quantity in the calculation of the absolute adsorption capacity of coal to the flue gas of a power plant. In the investigation of the adsorption mechanism of coal for power plant flue gas, it furnishes a data foundation for the precise analysis of experimental data, contributing to a more accurate understanding of the underlying principles (see Tables 6−8).

Table 6. Absolute Adsorption Capacity at 29.4 °C under Different Pressures

29.4 °C	absolute adsorption capacity V_{ad} (cm^3/g)				
P	RK	SRK	PR	LEE	BEB
0.168	0.798	0.7964	0.7892	0.7959	0.7737
0.954	8.3552	8.3309	8.4979	8.3698	10.3087
1.946	6.6896	6.5355	6.6717	6.634	9.2032
3.04	5.6715	5.6407	5.7831	5.6787	8.2601
4.165	4.6162	4.6861	4.8193	4.6763	6.881
4.957	4.0335	3.8075	3.864	3.933	6.8691

Table 7. Absolute Adsorption Capacity at 49.7 °C under Different Pressures

49.7 °C	Absolute adsorption capacity V_{ad} (cm^3/g)				
P	RK	SRK	PR	LEE	BEB
0.163	0.8875	0.8861	0.8798	0.8852	0.8744
1.117	3.737	3.6927	3.7839	3.7314	5.0496
1.882	3.197	3.169	3.2534	3.1996	4.6009
2.824	2.6639	2.6822	2.769	2.6911	4.2957
3.959	2.1507	2.2142	2.302	2.2022	4.0599
4.975	1.8432	1.7925	1.8472	1.8283	4.2352

Based on the data presented in Table 8 and the subsequent analysis, the Beggs−Brill algorithm is found to have the most ideal fitting effect at 29.4 °C according to the fitting precision R^2, and the fitting accuracy reaches 0.9954. At 49.7 °C, the PR gas equation of state is the most ideal, and the fitting accuracy reaches 0.977. The fitting results of the adsorbed molar phase under 29.4 °C are better than those under 49.7 °C. At 49.7 °C, the difference in the fitting accuracy of the adsorption phase

Table 8. Freundlich Equation Adsorption Fitting

T	29.4 °C					49.7 °C				
Z	RK	SRK	PR	LEE	BEB	RK	SRK	PR	LEE	BEB
k	0.003453	0.003471	0.003579	0.003479	0.004078	0.001572	0.001591	0.001641	0.001592	0.001235
$1/a$	0.7187	0.7113	0.7206	0.7177	1.089	0.5947	0.5917	0.6069	0.5965	1.438
R^2	0.983	0.9758	0.9755	0.9802	0.9954	0.9763	0.975	0.977	0.9766	0.9728

Table 9. Langmuir Equation Adsorption Fitting

T	29.4 °C					49.7 °C				
Z	RK	SRK	PR	LEE	BEB	RK	SRK	PR	LEE	BEB
A	0.2239	0.2326	0.2274	0.227	0.1235	0.5106	0.5156	0.4977	0.5093	0.2161
B	−0.02114	−0.03163	−0.02891	−0.02549	0.05579	−0.1843	−0.1927	−0.1813	−0.186	0.05548
R^2	0.9017	0.8894	0.8833	0.8953	0.8633	0.9263	0.9137	0.9111	0.9195	0.9748

obtained by the five compression factor calculation methods for the Freundlich equation is lower than 0.04. The Beggs−Brill algorithm can be used to predict the adsorption phase.

3.2.2. Adsorption Isothermal Curve Fitting. In the fitting of absolute adsorption capacity, the Langmuir equation was first used to compare the fitting of different absolute adsorption capacities, and the fitting parameters and fitting results are shown in Table 9 and Figures 13−17. The Langmuir
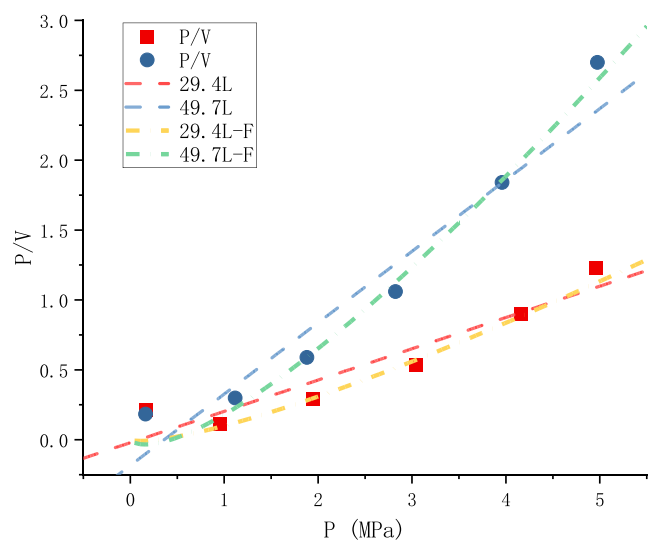
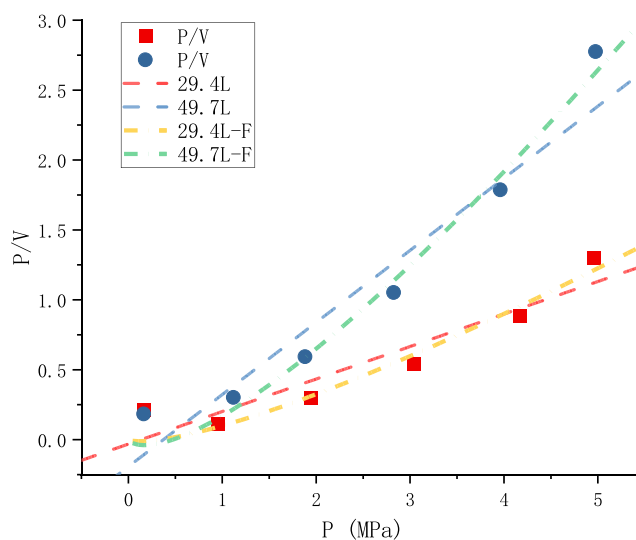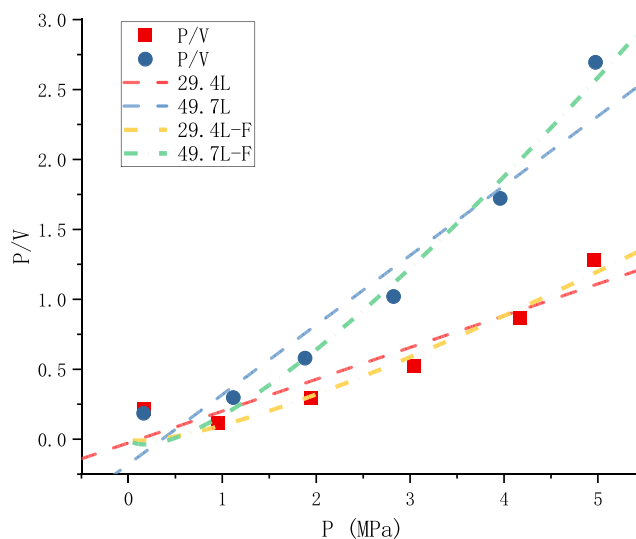**Figure 13.** RK equation fits the L equation and the L−F equation.

equation,[24] one of the commonly used adsorption isotherm equations, was proposed by physical chemist Langmuir Itying in 1916 on the basis of molecular motion theory and some assumptions and is now widely used in the calculation of adsorption equations. Its expression is

$$V = \frac{V_L b p}{1 + b p}$$

where V is the adsorption amount at adsorption equilibrium, cm³/g; V_L is the Langmuir volume, cm³/g; b is a constant, 1/Mpa; and P is the adsorption equilibrium pressure, Mpa.

To improve the accuracy of fitting, the above formula is transformed into a one-variable function

$$\frac{P}{V} = \frac{1}{b V_L} P + \frac{1}{V_L}$$

Figure 14. SRK equation fits the L equation and the L−F equation.

Figure 15. PR equation fits the L equation and the L−F equation.

In the expression, let $A = \frac{1}{b V_L}$ and $B = \frac{1}{V_L}$.

Because the fitting accuracy of the Langmuir equation was low, different adsorption capacities were substituted into the Langmuir−Freundlich equation for fitting. The fitting parameters and fitting results are shown in Table 10 and
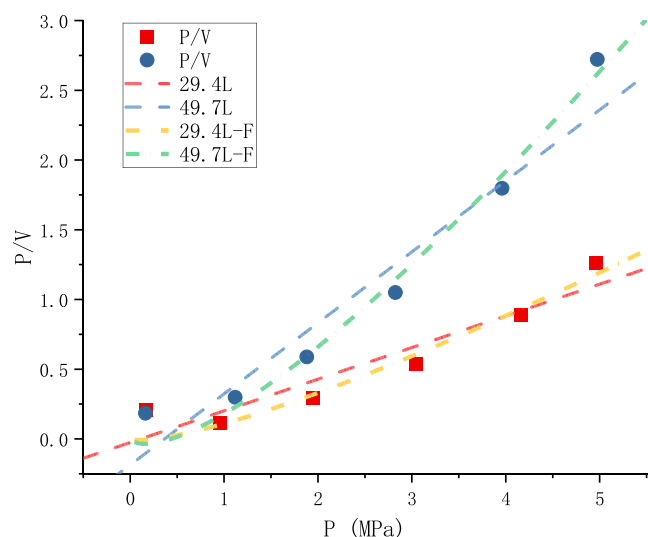
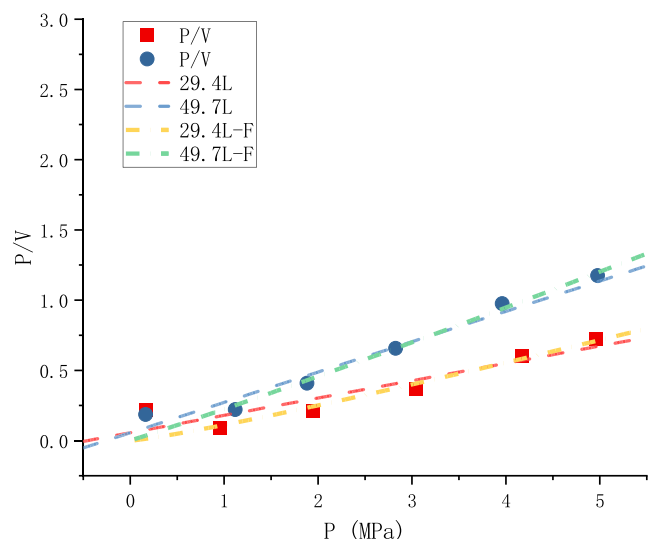**Figure 16.** LEE equation fits the L−equation and the L−F equation.

Figure 17. BEB equation fits the L equation and the L−F equation.

Figures 13−17. The Langmuir−Freundlich equation[25] is a semiempirical equation. This equation is based on the Langmuir equation, and an exponential Freundlich equation is introduced to represent the surface heterogeneity of the adsorbent. The expression is as follows

$$V = \frac{bV_L P^m}{1 + bP^m}$$

where V is the adsorption amount at adsorption equilibrium, cm^3/g; V_L is the Langmuir volume, cm^3/g; b is a constant, $1/$

Mpa; P is the adsorption equilibrium pressure, Mpa; and m is the parameter indicating the heterogeneity of the coal sample.

To improve the accuracy of fitting, the formula is rewritten as a power function of one variable

$$\frac{P}{V} = \frac{1}{bV_L}P^{1-m} + \frac{1}{V_L}P$$

In the expression, let $A = \frac{1}{bV_L}$; $B = \frac{1}{V_L}$; $1 - m = M$.

As evident from Tables 9 and 10 as well as Figures 13 and 17, the fitting performance of both the Langmuir equation and the Langmuir−Freundlich equation notably improves with an increase in temperature. At 29.4 °C, the fitting accuracy of the Langmuir equation and the Langmuir−Freundlich equation is suboptimal. However, at 49.7 °C, while the fitting accuracy of the Langmuir equation remains relatively low, the Langmuir−Freundlich equation, particularly when coupled with the RK, SRK, PR, and LEE equations, attains an accuracy exceeding 0.93, indicating a good fitting effect. Consequently, the Langmuir equation is deemed unsuitable for predicting the theoretical model of power plant flue gas adsorption capacity, whereas the Langmuir−Freundlich equation proves to be more appropriate for calculating the adsorption model of power plant flue gas.

3.2.3. Multimolecular Adsorption Model Fitting. On the basis of the Langmuir theoretical adsorption model, considering the flue gas of a power plant as a mixed gas, different absolute adsorption capacities were used for the Brunauer−Emmett−Teller (BET) multimolecular adsorption model. However, the common model in the BET multimolecular adsorption model can be divided into a two-parameter BET model and three-parameter BET model. The parameters and fitting results obtained by the two models are shown in Tables 11, 12 and Figures 18−22. The BET multimolecular adsorption model[26] is a multimolecular layer model proposed by BET based on the Langmuir model. Its main assumptions are as follows: there are van der Waals forces between molecules, which is not a simple monolayer adsorption; there is adsorption heat in the adsorption process of molecules, and the adsorption heat of each layer is different. The adsorption process occurs only on the surface of the gas phase.

1. The BET model expression for the two parameters is as follows

$$V = \frac{aCx}{(1-x)(1-x+Cx)}$$

where $x = \frac{P}{P_s}$; n is the adsorption amount at adsorption equilibrium, cm^3/g; p_s is the saturated vapor pressure, MPa; P is the adsorption equilibrium pressure, MPa; and C is the model parameter related to temperature and pore distribution.

In this paper, the empirical calculation formula of virtual saturated vapor pressure under supercritical conditions

Table 10. Langmuir−Freundlich Equation Adsorption Fitting

T	29.4 °C					49.7 °C				
Z	RK	SRK	PR	LEE	BEB	RK	SRK	PR	LEE	BEB
A	−37.55	−69.48	−62.17	−66.68	−4.628	−15.95	−19.06	−19.1	−18	0.007585
B	37.65	69.58	62.27	66.79	4.74	16.13	19.23	19.27	18.18	0.2164
M	0.9979	0.9987	0.9986	0.9988	0.9958	0.9867	0.9882	0.9886	0.9879	1.716
R^2	0.942	0.9362	0.931	0.9389	0.8521	0.9858	0.9809	0.9792	0.9832	0.9652

Table 11. BET Two-Point Model Adsorption Fitting

T	29.4 °C					49.7 °C				
Z	RK	SRK	PR	LEE	BEB	RK	SRK	PR	LEE	BEB
A	2541	2418	2371	2508	1501	9579	5511	8213	5693	4738
C	0.03876	0.04007	0.04159	0.03944	0.09997	0.001467	0.002519	0.001748	0.002469	0.006191
R^2	0.9264	0.9382	0.9366	0.933	0.7563	0.934	0.9433	0.9426	0.9391	0.6437
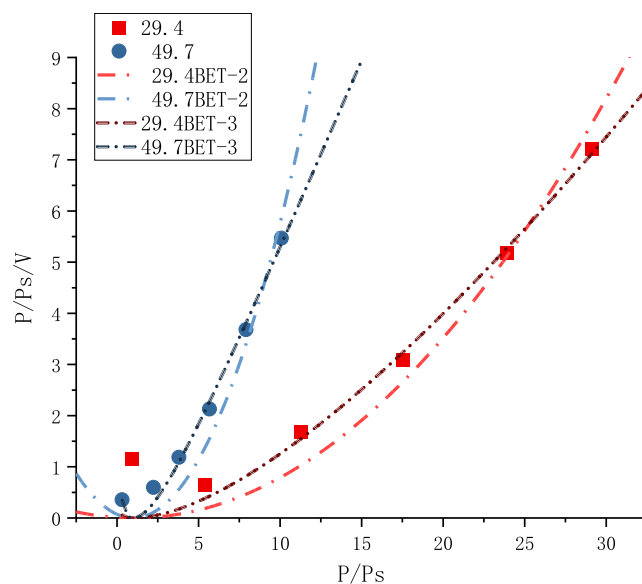
Figure 18. RK equation fits the BET model.
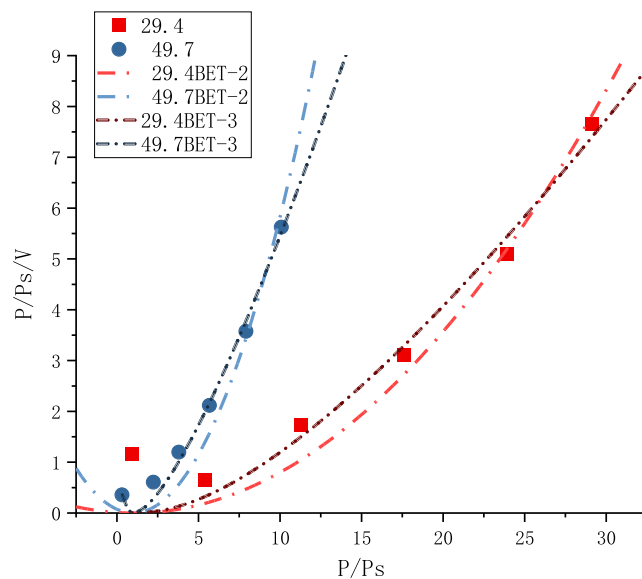
Figure 19. SRK equation fits the BET model.

established by Dubinin (Dubinin, 1960)[27] is used to calculate the saturated vapor pressure. The calculation formula is

$$P_S = P_C \left(\frac{T}{T_c} \right)^2$$

2. BET model with three parameters

$$V = \frac{aCx}{(1-x)} \times \frac{1 - (m+1)x^m + mx^{m+1}}{1 + (C-1)x - Cx^{m+1}}$$

where $x = \frac{P}{p_s}$; n is the adsorption amount at adsorption equilibrium, cm^3/g; p_s is the saturated vapor pressure, MPa; P is the adsorption equilibrium pressure, MPa; C is the model parameter related to temperature and pore distribution; and m is a constant.

The analysis of Tables 11 and 12, as well as Figures 18 and 22, reveals the following: in the BET adsorption model, the
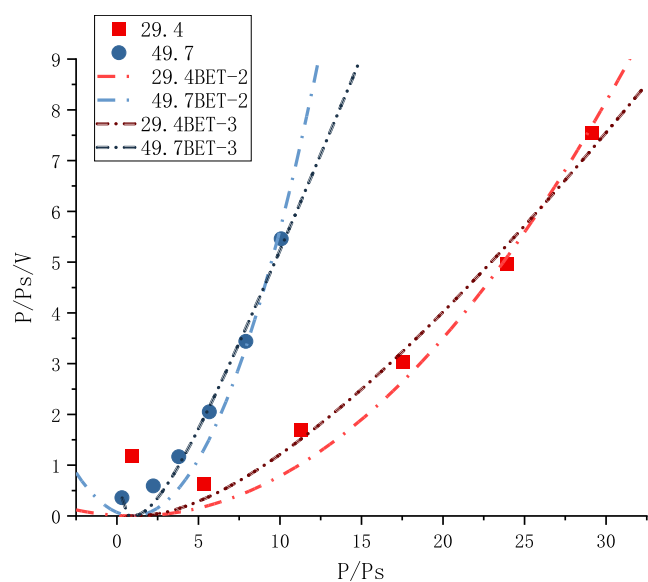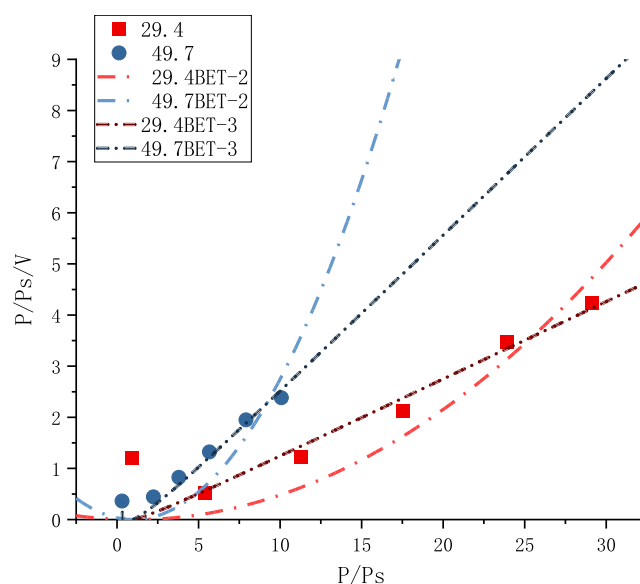
Figure 20. PR equation fits the BET model.

Figure 22. BEB equation fits the BET model.
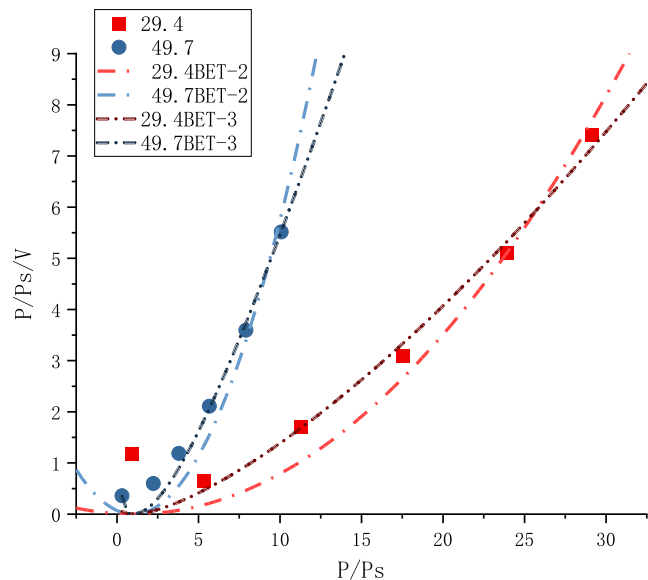

Figure 21. LEE equation fits the BET model.

fitting results of the three-parameter BET adsorption model are obviously better than those of the two-parameter BET adsorption model, and the fitting results of the three-parameter BET adsorption models by RK, SRK, PR, and LEE calculations of compression factors are all above 0.9487 at the two temperatures. Therefore, the three-parameter BET adsorption model is more suitable for predicting the adsorption capacity of power plant smoke than the two-parameter BET adsorption model. At 29.4 °C, the two forms of BET model fit are too low, both exceeding 0.944. At 49.7 °C, the BET model with three parameters of the RK equation of state has a higher fitting degree. The RK equation has the best fitting effect, and the fitting accuracy R^2 is up to 0.9922. At about 50 °C, the adsorption model of three parameters of BET has an excellent fitting effect.

3.2.4. Adsorption Potential Model Fitting. Finally, different absolute adsorption capacities were fitted and compared with the Dubinin−Radushkevich equation adsorption potential

theoretical model, and the fitting parameters and fitting results are shown in Table 13 and Figures 23−27. The principal distinction between adsorption potential theory and the Langmuir single molecular layer and BET multimolecular layer adsorption theories lies in its premise that there exists an adsorption potential field on the solid surface. According to this theory, the farther away from the solid surface, the lower the adsorption potential energy, consequently influencing the density of the adsorption phase in relation to the distance from the surface. Dubinin et al. incorporated the adsorption potential theory into the study of pore adsorption, asserting that the gas adsorption behavior within the adsorbent entails pore filling rather than surface covering. The expression for this theory is detailed in ref 27

$$V = V_0 \exp\left[-D \ln^2\left(\frac{P_s}{P}\right)\right]$$

where $D = \frac{RT}{\beta E}$; V is the adsorption capacity, cm^3/g; p_s is the saturated vapor pressure, Mpa; and P is the adsorption pressure, MPa.

The different compression factors and adsorption capacity calculated by MATLAB were substituted into the Dubinin−Radushkevich equation for fitting parameters and fitting results, as shown in Table 13.

As evident from Table 10, Figures 23 and 27, the difference in fitting accuracy obtained by the DR model under two experimental temperatures is not uniform. The fitting accuracy of RK, SRK, PR, and LEE compression factor calculation methods at 29.4 °C is lower than that at 49.7 °C, but the fitting degree can reach more than 0.945 at both temperatures. The BEB method showed the opposite trend to the first four methods, and the highest fitting degree was only 0.8797.

3.2.5. Theoretical Adsorption Model Analysis. With the fitting precision R^2 as the criterion, the most accurate model was selected from the cross combination of the above five compression factor calculation methods and the five absolute adsorption calculation fitting models. By comparing the fitting accuracy R^2, the optimal adsorption prediction model should be selected for the RK gas state equation and BET theoretical

Table 12. BET Three-Point Model Adsorption Fitting

T	29.4 °C					49.7 °C				
Z	RK	SRK	PR	LEE	BEB	RK	SRK	PR	LEE	BEB
a	5876	961.7	532	1729	386,400	1.524	0.9501	2.15	5.097	0.1042
C	−570.3	−117.3	−66.39	−188.9	−9842	−1.509	0.9934	−1.771	−3.274	−1.98
m	0.0046	0.009359	0.015	0.007807	0.5873	1.328	−0.6341	1.023	0.5612	61.8
R^2	0.9547	0.9525	0.9487	0.9535	0.9147	0.9922	0.9824	0.9867	0.9867	0.9723

Table 13. Dubinin−Radushkevich Equation Adsorption Fitting

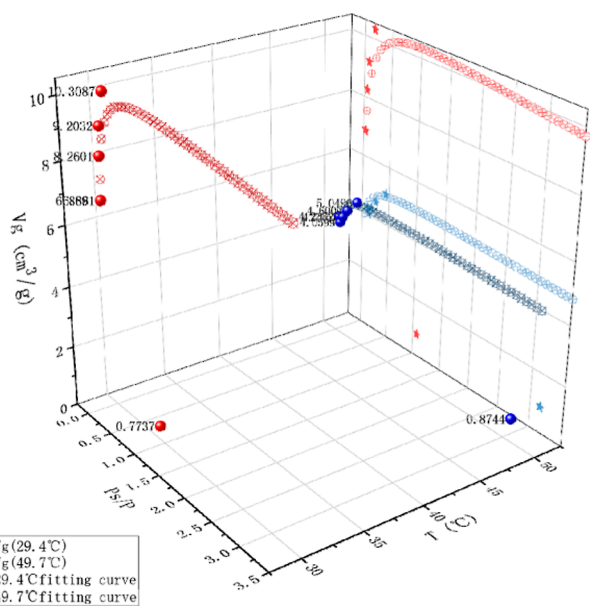| T	29.4 °C					49.7 °C				
Z	RK	SRK	PR	LEE	BEB	RK	SRK	PR	LEE	BEB
V_0	8.361	8.337	8.504	8.376	10.31	3.663	3.725	3.726	3.666	5.059
D	0.314	0.316	0.3119	0.3143	0.1988	0.2794	0.3269	0.2689	0.2751	0.1518
R^2	0.9453	0.9462	0.945	0.9456	0.8797	0.9777	0.9523	0.9743	0.9778	0.8284

Figure 23. RK equation fits the DR model.

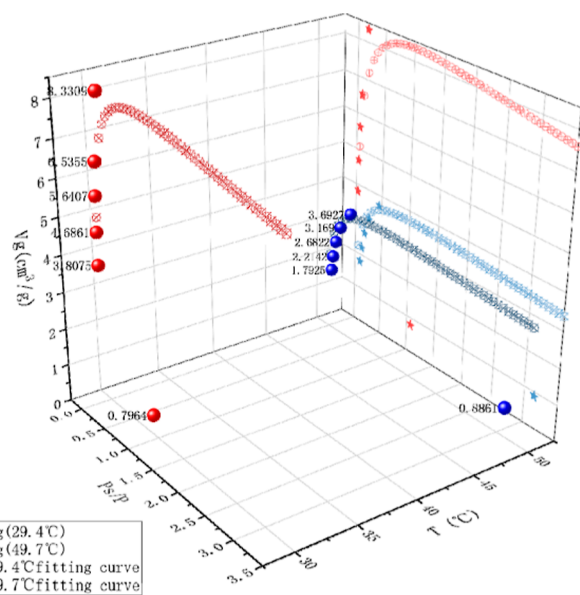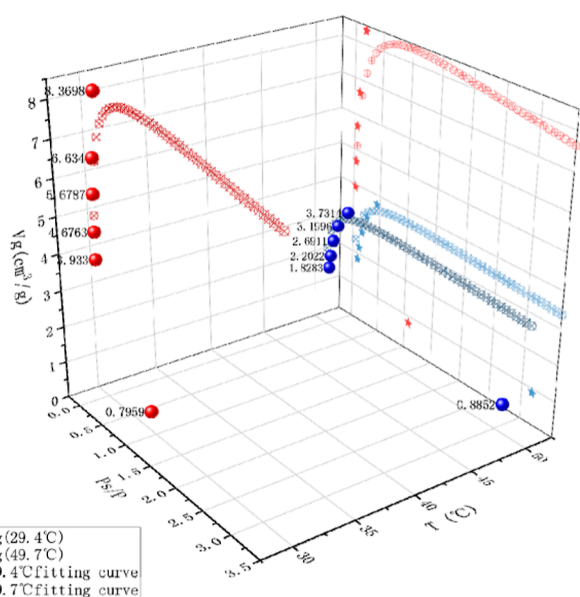**Figure 25.** PR equation fits the DR model.
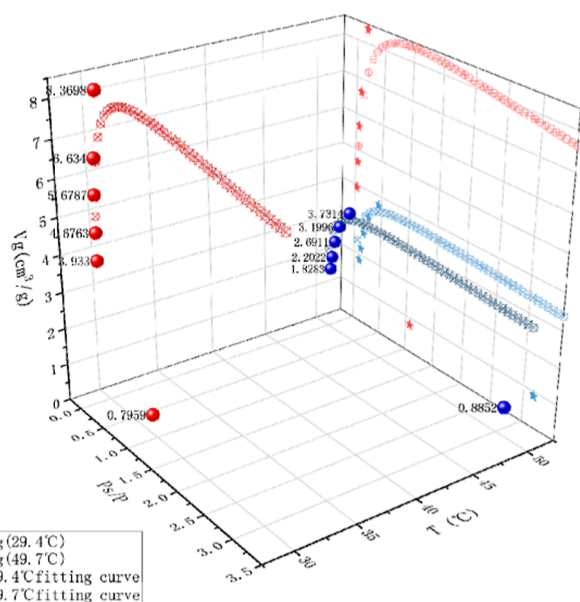

Figure 24. SRK equation fits the DR model.

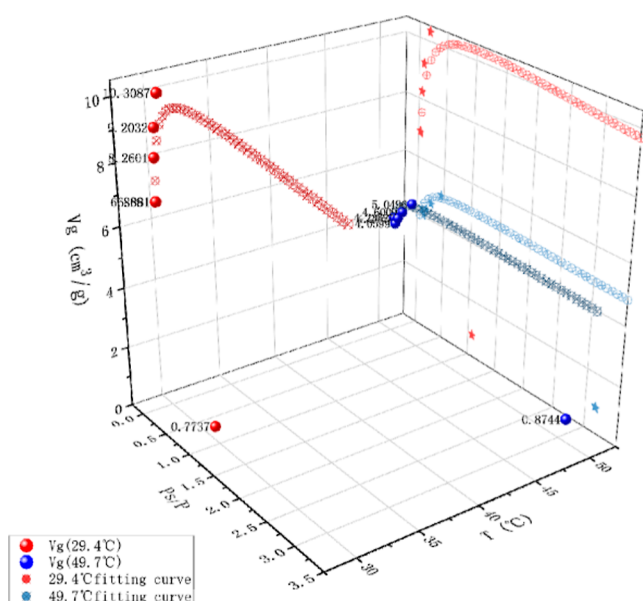**Figure 26.** LEE equation fits the DR model.

Figure 27. BEB equation fits the DR model.

adsorption prediction model with three parameters. Therefore, by substituting the fitting coefficient obtained from the RK equation of state in Table 12 into the BET theoretical adsorption prediction model, two prediction calculation models of gas adsorption capacity at 29.4 and 49.7 °C can be obtained, as shown below.

At 29.4 °C, the coal flue gas adsorption prediction model for power plants is expressed as

$$V = \frac{-3351082.8x}{(1-x)} \times \frac{1 - (1.0046)x^{0.0046} + 0.0046x^{1.0046}}{1 + (-571.3)x + 570.3x^{1.0046}}$$

At 49.7 °C, the flue gas adsorption prediction model for coal in power plants is given by

$$V = \frac{2.299716x}{(1-x)} \times \frac{1 - (2.328)x^{1.328} + 1.328x^{2.328}}{1 + (-2.509)x + 1.509x^{2.328}}$$

It can be observed from the fitting results of the above five theoretical adsorption models on absolute adsorption capacity that the Beggs−Brill method is not suitable for calculating the adsorption capacity of coal to power plant flue gas. It can be seen from Tables 3 and 4 that there is a slight error in the absolute adsorption volume obtained by different compression factor calculation methods. However, because of the small unit scale of the results obtained by the experimental system, the error will be exponentially amplified with the increase in the unit index in actual production and application. Through the fitting calculation of the above theoretical adsorption model, the most suitable compression factor calculation method is verified, and the error in the calculation of the coal gas adsorption capacity of the power plant is reduced as much as possible, which will have a relatively important significance for the future gas storage of the power plant and coal bed methane (CBM) displacement.

4. CONCLUSIONS

In this study, we conducted a flue gas adsorption experiment on coal samples from the Zhaozhuang no. 2 well within a power plant setting. The compression factor coefficients were calculated using five gas state equations, and the resulting absolute adsorption capacities under various compression factor calculation methods were fitted to six adsorption models. This process aimed to identify the most suitable calculation model. The theoretical adsorption model proposed in this paper serves as a robust foundation for predicting flue gas adsorption capacity and CBM displacement in moth bated power plants located within abandoned coal mines. The key conclusions are as follows

1. The absolute adsorption volume error ranges for RK, SRK, PR, and Lee compression factor calculation methods are 0.069−0.226 cm^3 at 29.4 °C and 0.004− 0.0547 cm^3 at 49.7 °C. The absolute adsorption volumes obtained from the Beggs−Brill method and the other four compression factor calculation methods exhibit significant errors at both temperatures, rendering them unsuitable for modeling coal flue gas adsorption in power plants.

2. The transformed form of the RK equation of state proves to be the most appropriate method for calculating the compression factor of coal samples from Zhaozhuang no. 2 well. The BET adsorption model, featuring three parameters, emerges as the most suitable theoretical adsorption model for these coal samples. At 29.4 and 49.7 °C, the BET adsorption model, coupled with the RK equation of state and three parameters, exhibits high fitting accuracy, reaching 0.9547 and 0.9922, respectively.

3. The optimal adsorption capacity prediction model at two different temperatures was obtained by substituting the fitting coefficient obtained in Table 12 into the BET adsorption model. At 29.4 °C, the coal flue gas adsorption prediction model for power plants is expressed as

$$V = \frac{-3351082.8x}{(1-x)} \times \frac{1 - (1.0046)x^{0.0046} + 0.0046x^{1.0046}}{1 + (-571.3)x + 570.3x^{1.0046}}$$

At 49.7 °C, the flue gas adsorption prediction model for coal in power plants is given by

$$V = \frac{2.299716x}{(1-x)} \times \frac{1 - (2.328)x^{1.328} + 1.328x^{2.328}}{1 + (-2.509)x + 1.509x^{2.328}}$$

■ AUTHOR INFORMATION

Corresponding Author

Gang Bai − *College of Safety Science & Engineering, Liaoning Technical University, Huludao, Liaoning 125105, China; Key Laboratory of Mine Thermodynamic Disasters & Control of Ministry of Education, Huludao, Liaoning 125105, China;* ⊙ orcid.org/0000-0002-4599-6388; Email: 1272661640@qq.com

Authors

Miaoxin Cheng − *College of Safety Science & Engineering, Liaoning Technical University, Huludao, Liaoning 125105, China;* ⊙ orcid.org/0009-0009-1021-3214

Hongbao Zhao − *School of Energy and Mining Engineering, China University of Mining and Technology (Beijing), Beijing 100083, China*

Jinyu Li − *College of Safety Science & Engineering, Liaoning Technical University, Huludao, Liaoning 125105, China; Key Laboratory of Mine Thermodynamic Disasters &*

Control of Ministry of Education, Huludao, Liaoning 125105, China

Jun Su − *College of Safety Science & Engineering, Liaoning Technical University, Huludao, Liaoning 125105, China*

Jue Wang − *College of Safety Science & Engineering, Liaoning Technical University, Huludao, Liaoning 125105, China*

Xun Zhang − *College of Mining, Liaoning Technical University, Fuxin 123000, China*

Complete contact information is available at:

https://pubs.acs.org/10.1021/acsomega.3c10005

Author Contributions

G.B. contributed equally to this work. Miaoxin Cheng: Investigation, Writing—original draft. Gang Bai: Conceptualization, Methodology, Investigation, Writing—original draft. Hongbao Zhao: Resources. Jinyu Li: Investigation. Jun Su: Resources. Jue Wang: Conceptualization, Methodology. Xun Zhang: Resources.

Notes

The authors declare no competing financial interest.

■ REFERENCES

(1) IEA. *Energy Technology Perspectives 2020: Special Report on Carbonapture, Utilization and Storage*; IEA: Paris, 2020.

(2) Jiachen, W.; Kretschmann, J.; Yang, L. Reflections on resource utilization and sustainable development of closed coal mining areas. *J. Min. Sci. Technol.* **2021**, *6* (6), 633−641.

(3) Larki, I.; Zahedi, A.; Asadi, M.; Forootan, M. M.; Farajollahi, M.; Ahmadi, R.; Ahmadi, A. Mitigation approaches and techniques for combustion power plants flue gas emissions: a comprehensive review. *Sci. Total Environ.* **2023**, *903*, 166108.

(4) Dutta, P.; Harpalani, S.; Prusty, B. Modeling of CO_2 sorption on coal. *Fuel* **2008**, *87* (10−11), 2023−2036.

(5) Pan, Z.; Connell, L. D. Comparison of adsorption models in reservoir simulation of enhanced coalbed methane recovery and CO2 sequestration in coal. *Int. J. Greenhouse Gas Control* **2009**, *3* (1), 77−89.

(6) Sakurovs, R.; Day, S.; Weir, S. Relationships between the sorption behavior of methane, carbon dioxide, nitrogen and ethane on coals. *Fuel* **2012**, *97*, 725−729.

(7) Lee, H.-H.; Kim, H.-J.; Shi, Y.; Keffer, D.; Lee, C.-H. Competitive adsorption of CO2/CH4 mixture on dry and wet coal from subcritical to supercritical conditions. *Chem. Eng. J.* **2013**, *230*, 93−101.

(8) Yang, Y.; Liu, S.; Zhao, W.; Wang, L. Intrinsic relationship between Langmuir sorption volume and pressure for coal: Experimental and thermodynamic modeling study. *Fuel* **2019**, *241*, 105−117.

(9) Qi, R.; Ning, Z.; Wang, Q.; Huang, L.; Wu, X.; Cheng, Z.; Zhang, W. Measurements and modeling of high-pressure adsorption of CH_4 and CO_2 on shales. *Fuel* **2019**, *242*, 728−743.

(10) Meng, M.; Qiu, Z.; Zhong, R.; Liu, Z.; Liu, Y.; Chen, P. Adsorption characteristics of supercritical CO_2/CH_4 on different types of coal and a machine learning approach. *Chem. Eng. J.* **2019**, *368*, 847−864.

(11) Kang, J.; Wan, R.; Zhou, F.; Liu, Y.; Li, Z.; Yin, Y. Effects of supercritical CO_2 extraction on adsorption characteristics of methane on different types of coals. *Chem. Eng. J.* **2020**, *388*, 123449.

(12) Mu, Y.; Fan, Y.; Wang, J.; Fan, N. Numerical study on injection of flue gas as a heat carrier into coal reservoir to enhance CBM recovery. *J. Nat. Gas Sci. Eng.* **2019**, *72*, 103017.

(13) Chen, X.; Zhao, S.; Li, L.; Li, X.; Kang, N. Effect of ambient pressure on gas adsorption characteristics of residual coal in abandoned underground coal mines. *J. Nat. Gas Sci. Eng.* **2021**, *90*, 103900.

(14) Liu, L.; Yang, M.; Zhang, X.; Mao, J.; Chai, P. LNMR experimental study on the influence of gas pressure on methane adsorption law of middle-rank coal. *J. Nat. Gas Sci. Eng.* **2021**, *91*, 103949.

(15) Liu, D.; Yao, Y.; Chang, Y. Measurement of adsorption phase densities with respect to different pressure: potential application for determination of free and adsorbed methane in coalbed methane reservoir. *Chem. Eng. J.* **2022**, *446* (Part 3), 137103.

(16) Cheng, X.; Cheng, Y.; Wang, C.; Hu, B.; Wang, J. Calculation methods on methane adsorption phase density in coal: a critical review and new insights. *Chem. Eng. J.* **2023**, *472*, 144778.

(17) Huang, M.C.; Yu, H.; Xu, H.Y.; Zhang, H.L.; Hong, X.Y.; Wu, H.A. Fast and accurate calculation on CO_2/CH_4 competitive adsorption in shale nanopores: from molecular kinetic theory to machine learning model. *Chem. Eng. J.* **2023**, *474*, 145562.

(18) Atkins, P.; Paula, J. d. *Atkins' Physical Chemistry*, 8th ed.; Oxford University Press, 2006.ISBN 9780198700722.

(19) Murdock, J. W. *Fundamental Fluid Mechanics for the Practicing Engineer*; CRC Press, 1993; pp 25−27.ISBN 0824788087.

(20) Smith, J. M.; Van Nes, H. C.; Abbott, M. M. *Introduction to Chemical Engineering Thermodynamics*; McGraw-Hill: New York, 2001.

(21) Prausnitz, J. M.; Gunn, R. D. Volumetric properties of nonpolar gaseous mixtures. *AIChE J.* **1958**, *4*, 430−435.

(22) Lee, B. I.; Kesler, M. G. A generalized thermodynamic correlation based on three-parameter corresponding states. *AIChE J.* **1975**, *21*, 510−527.

(23) Freundlich, H. Uber die adsorption in losungen. *Z. Phys. Chem.* **1907**, *57U*, 385−470.

(24) Langmuir, I. The constitution and fundamental properties of solid sand liquids. II. Liquids. *J. Franklin Inst.* **1916**, *184* (5), 102−105.

(25) Markham, E. C.; Benton, A. F. The adsorption of gas mixtures by silica. *J. Am. Chem. Soc.* **1931**, *53* (2), 497−507.

(26) Dubinin, M. M. Fundamentals of the theory of adsorption in micropores of carbon adsorbents: characteristics of their adsorption properties and microporous structures. *Carbon* **1989**, *27* (3), 457−467.

(27) Dubinin, M. M. The potential theory of adsorption of gases and vapors for adsorbents with energetically nonuniform surfaces. *Chem. Rev.* **1960**, *60*, 235−241.